Discriminant Function of Optical Coherence Tomography Angiography to Determine Disease Severity in Glaucoma

Rajesh S. Kumar,[*,1] Neha Anegondi,[2] Rachana S. Chandapura,[2] Suria Sudhakaran,[1] Sujatha V. Kadambi,[1] Harsha L. Rao,[1] Tin Aung,[3,4] and Abhijit Sinha Roy[2]

[1]Narayana Nethralaya Eye Hospital, Bangalore, India
[2]Imaging, Biomechanics and Mathematical Modeling Solutions, Narayana Nethralaya Foundation, Bangalore, India
[3]Singapore Eye Research Institute and Singapore National Eye Center, Singapore
[4]Yong Loo Lin School of Medicine, National University of Singapore, Singapore

Correspondence: Rajesh S. Kumar, Glaucoma Services, Narayana Nethralaya, 121/C, Chord Road, 1 'R' Block, Rajajinagar, Bangalore 560 010, Karnataka, India; raj_skumar@yahoo.com.

Current affiliation: *Cleveland Clinic Eye Institute, Abu Dhabi, UAE.

Submitted: May 24, 2016
Accepted: October 9, 2016

Citation: Kumar RS, Anegondi N, Chandapura RS, et al. Discriminant function of optical coherence tomography angiography to determine disease severity in glaucoma. *Invest Ophthalmol Vis Sci*. 2016;57:6079–6088. DOI:10.1167/iovs.16-19984

Purpose. To determine the discriminant function of optical coherence tomography angiography (OCTA) by disease severity in glaucoma.

Methods. In this prospective, observational cross-sectional study, all subjects underwent visual fields, retinal nerve fiber layer (RNFL) measurements, and OCTA imaging. Local fractal analysis was applied to OCTA images (radial peripapillary capillaries [RPC] layer). Vessel density en face and inside the disc and spacing between large and small vessels were quantified. Stepwise logistic regression was performed and a glaucoma severity score (range, 0–1: 0, normal; 1, severe glaucoma) was developed by using global and regional (superotemporal [ST], inferotemporal [IT], temporal, superonasal [SN], inferonasal, and nasal) vascular parameters. Glaucoma severity score was compared with visual field and RNFL indices.

Results. One hundred ninety-nine eyes (112 subjects) with glaucoma (28 eyes preperimetric; 83 early, 43 moderate, and 45 severe glaucoma) and 74 normal (54 subjects) eyes were enrolled. Preperimetric and glaucomatous eyes had significantly altered ($P < 0.001$) global vascular parameters as compared to normal; regionally, ST, then SN and IT sectors (in that order) showed more change in glaucomatous eyes. Vascular parameters showed better discriminant ability (area under the curve [AUC], sensitivity, and specificity of 0.70, 69.2%, and 72.9%, respectively) than structural parameters between normal and preperimetric glaucomatous eyes. Vascular parameters had comparable AUC ($P > 0.05$) to visual fields for perimetric glaucoma. Glaucoma severity score identified preperimetric glaucoma and early glaucoma better than did visual fields.

Conclusions. Vascular parameters could be a useful adjunct tool to evaluate/diagnose glaucoma. Longitudinal studies are needed to determine their use in early detection and prognostication.

Keywords: optical coherence tomography, glaucoma, visual field, angiography

Glaucoma is the leading cause of irreversible blindness worldwide.[1,2] It is characterized by progressive degeneration of the optic nerve and loss of retinal ganglion cells, with corresponding visual field (VF) defects on standard automated perimetry.[1,2] While raised intraocular pressure (IOP) is currently the only known modifiable risk factor for glaucoma, there is evidence that vascular insufficiency in the optic nerve head (ONH) also plays an important role in the pathogenesis of glaucoma.[3–5] Currently, a number of methods are available for measuring ONH perfusion.[6–11] Fluorescein angiography is invasive. It provides only superficial ONH perfusion and not deep perfusion.[6] Noninvasive methods such as laser Doppler flowmetry and laser speckle flowgraphy have demonstrated decreased ONH perfusion in glaucomatous eyes, but have moderate repeatability.[8,10] Doppler OCT can quantify retinal blood flow around the ONH in large vessels; however, microcirculation cannot be accurately determined.[11]

Optical coherence tomography angiography (OCTA) is a recent, noninvasive imaging technique for evaluating the ONH vascular network.[12] Several recent studies[7,13–15] have shown the utility of OCTA in determining the changes in ONH perfusion with increasing severity of glaucoma. In recent studies,[16,17] a local fractal-based method has been used to determine the presence or absence of vessels in OCTA images. Vascular parameters, such as vessel density, regions with no or minimal vascular features, and regions surrounding small vessels, have been quantified.[16,17] The method is not device specific and not limited to just OCTA images.[16,17] In this study, global and regional differences in vascular parameters around the ONH were evaluated in normal, preperimetric, and glaucomatous eyes. Further, the study attempted to determine the discriminant capacity of the vascular parameters, on the basis of disease severity, and compared it with the discriminant capacity of VFs, retinal nerve fiber layer thickness (RNFLT), and ganglion cell complex (GCC) thickness.

Methods

This was a prospective, cross-sectional, observational study conducted on consecutive Indian subjects attending the glaucoma clinic of a tertiary eye care center from May 2015

to November 2015. Informed consent was obtained from all participants and the Ethics Committee of the institute approved the study. The study adhered to the tenets of the Declaration of Helsinki for research involving human subjects.

Overall inclusion criteria were age greater than or equal to 18 years, best corrected distance visual acuity of 20/40 or better, and refractive error within ±5–diopter (D) sphere and ±3-D cylinder. Exclusion criteria were presence of any media opacities that prevented good quality optic disc photographs and other imaging tests, and any ocular disease (including uveitis, macular, or neurologic) other than glaucoma, which could confound the evaluations. All participants underwent a comprehensive ocular examination, which included a detailed medical history, best corrected distance visual acuity measurement, slit-lamp biomicroscopy, Goldmann applanation tonometry for IOP, 4-mirror gonioscopy, dilated fundus examination, VF examination, stereoscopic optic disc photography (Kowa Company, Ltd., City, Japan), and OCTA imaging using spectral-domain optical coherence tomography (SD-OCT, RTVue-XR; Optovue, Inc., Fremont, CA, USA).

Preperimetric glaucomatous subjects had normal VF but glaucomatous ONH changes. Those with perimetric glaucoma had characteristic glaucomatous VF loss and corresponding ONH changes. Glaucomatous VF loss was defined as a repeatable field that showed pattern standard deviation (PSD) less than 5% and a glaucoma hemifield test outside normal limits on the Humphrey Swedish interactive thresholding algorithm (SITA) standard 24-2 VF. Optic nerve head changes were termed as thinning, notching, optic nerve hemorrhage, cup/disc (C/D) asymmetry greater than 0.2, and focal nerve fiber layer defects. This was based on stereoscopic ONH assessment by a glaucoma-trained specialist masked to other clinical findings. Perimetric glaucomatous eyes were graded as early, moderate, and severe based on the Hodapp, Parish, and Anderson (HPA) classification system.[18] The HPA classification considered (1) the extent of overall damage using mean deviation (MD) value and (2) the number of defective points in the pattern deviation map of 24-2 SITA standard VF test.[17] Only primary glaucomatous eyes were included. An eye with open angle glaucoma had open angles, ONH defects, and VF defects characteristic of glaucoma. Eyes with primary angle closure glaucoma (PACG) had at least 180° of nonvisualization of posterior trabecular meshwork on gonioscopy along with ONH and corresponding VF changes. Patients with any other ocular disease other than primary glaucoma were excluded from the study. Normal subjects had an IOP less than or equal to 21 mm Hg, normal fields, a normal-appearing ONH, RNFL, and open angles.

Visual Field Examination

Standard VF testing was performed by using standard automated perimetry (Humphrey SITA standard 24-2 protocol; Carl Zeiss Meditec, Dublin, CA, USA). The VF was considered reliable for a fixation loss of less than 20% with false-positive and false-negative errors less than 15%. The mean global sensitivity of the VF was expressed as MD (in dB) and PSD (in dB). Regional VF loss was determined by total deviation and pattern deviation maps, which identified abnormal regions of the field relative to an age-matched population.

Retinal Nerve Fiber Layer and GCC Measurements

The mean RNFL and GCC thicknesses were measured by using RTVue-XR. Retinal nerve fiber layer thickness was determined in ONH mode in which data along a 3.45-mm-diameter circle around the optic disc was mapped by using 12 concentric rings and 24 radial scans. Mean, superior, and inferior RNFL thicknesses were computed. The GCC scan covered a square grid of 6 × 6 mm on the central macula and was centered 1 mm temporal to the fovea. The GCC thickness was measured from the inner limiting membrane (ILM) to the posterior boundary of the inner plexiform layer. Mean, superior, and inferior GCC thicknesses were acquired. In addition, two pattern-based diagnostic parameters, focal loss volume (FLV as %) and global loss volume (GLV as %), were also computed. A single experienced operator acquired all scans. The operator was blinded to all the clinical data.

Vascular Parameters

The OCTA images (4.5 × 4.5 mm) generated from the radial peripapillary capillaries (RPC) layer of the ONH had a complex and dense microvasculature. To generate the OCTA images of the RPC layer, the segmentation boundary extended from the ILM to the outer boundary of nerve fiber layer. To analyze the local variations in vasculature, local fractal method was used. Box-counting method given by Equation 1 was used to calculate the fractal dimension:

$$Fractal\ Dimension = \frac{\log(N_b)}{\log(b)}. \quad (1)$$

In Equation 1, N_b was the number of boxes of magnification (b) needed to enclose the structure in the image. A modified box-counting method using a moving window of size (2w + 1) × (2w + 1) given by Equation 2 was used to calculate the local fractal dimension of each pixel in the image[17,19]:

$$G(i,j) = Local\ Fractal\ Dimension\ [I(i+k,j+k); -w<k<w]. \quad (2)$$

G was the new image obtained from the original image I after replacing the center pixel of each window with the fractal dimension of the window. A window size of 3 × 3 pixels was found to be suitable to calculate the local fractal dimension.[16,17] Each pixel in the OCTA image was assigned a local fractal dimension value obtained from Equation 2. However, the magnitude of fractal dimension of each pixel varied with the distribution of the surrounding vascular network.[19] Thus, a pixel within a large vessel had a higher fractal dimension than a pixel located in a small vessel or a nonvascular region.[16,17] A normalized fractal dimension ratio was computed for each pixel by taking the ratio of its local fractal dimension with the maximum computed local fractal dimension in the image, G.[16,17] The normalized ratio was plotted as a 2-D contour map that gave pictorial representation of the presence of a given pixel in the OCTA image within a vessel or a nonvascular region of the image. Therefore, a normalized ratio closer to 1 indicated a vessel and a ratio closer to 0 indicated a nonvessel region.[16,17] A scoring system was developed from visual examination of the normalized ratio map with the OCTA image.[16,17] The pixels within the large vessels had a normalized ratio between 0.9 and 1.0, while the pixels within the small vessels had a ratio between 0.7 and 0.9.[16,17] Anatomically, "large vessels" indicated retinal arterioles and venules and "small vessels" indicated capillaries. Pixels in regions that were devoid or had minimal vascular features had a normalized ratio between 0.0 and 0.3.[16,17] By visual observation, these were often observed to be in regions between or around large vessels and sometimes between widely spaced small vessels. In general, these were termed as "spaces between large vessels." Pixels in regions around small vessels, which may be branching out from a large vessel or surrounding small vessels, had a normalized ratio between 0.3 and 0.7.[16,17] These were termed as "spaces between small

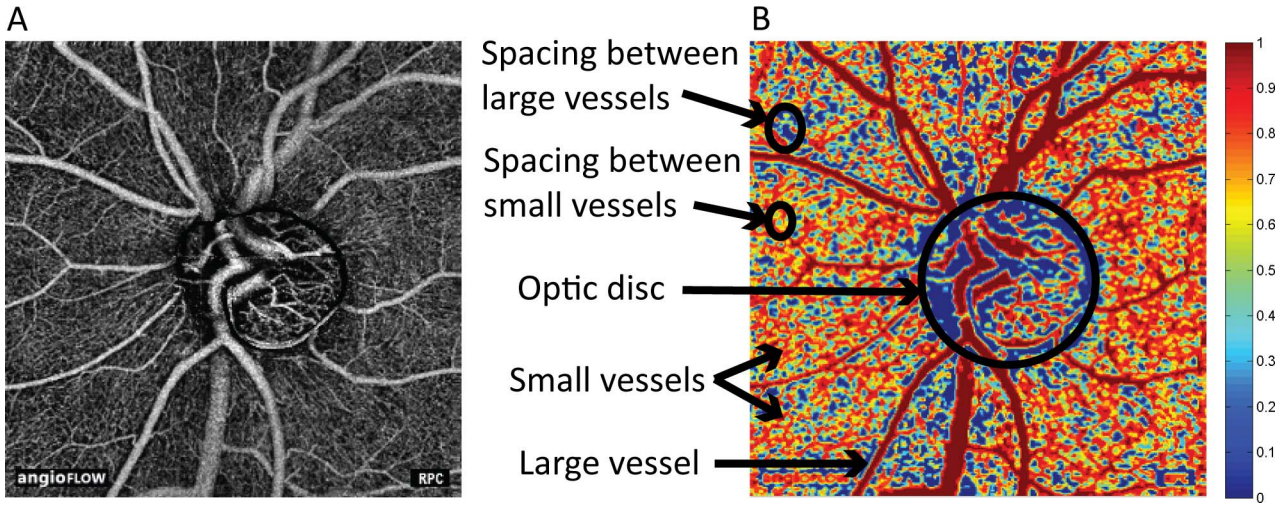

Figure 1. (**A**) Optical coherence tomography angiography of RPC layer of glaucomatous eye. (**B**) Corresponding contour map with the marked and labeled optic disc and examples of large vessel, small vessels, spacing between large vessels, and spacing between small vessels.

vessels" and were generally observed in closely packed clusters of vessels. The ONH was segmented by using boundary detection (MathWorks, Inc., Natick, MA, USA).

Figures 1A and 1B show the original OCTA image of the RPC layer of a glaucomatous eye and the corresponding contour map, respectively. The figures also show the optic disc with examples of large vessel, small vessel, spacing between large vessels, and spacing between small vessels. Figures 2A through 2D show the RNFLT, GCC thickness, VF distribution, structural OCT image, and original en face OCTA image of the RPC layer of a preperimetric, early, moderate, and severe glaucomatous eye, respectively. The corresponding contour maps of normalized local fractal dimension derived from the OCTA image are also shown.

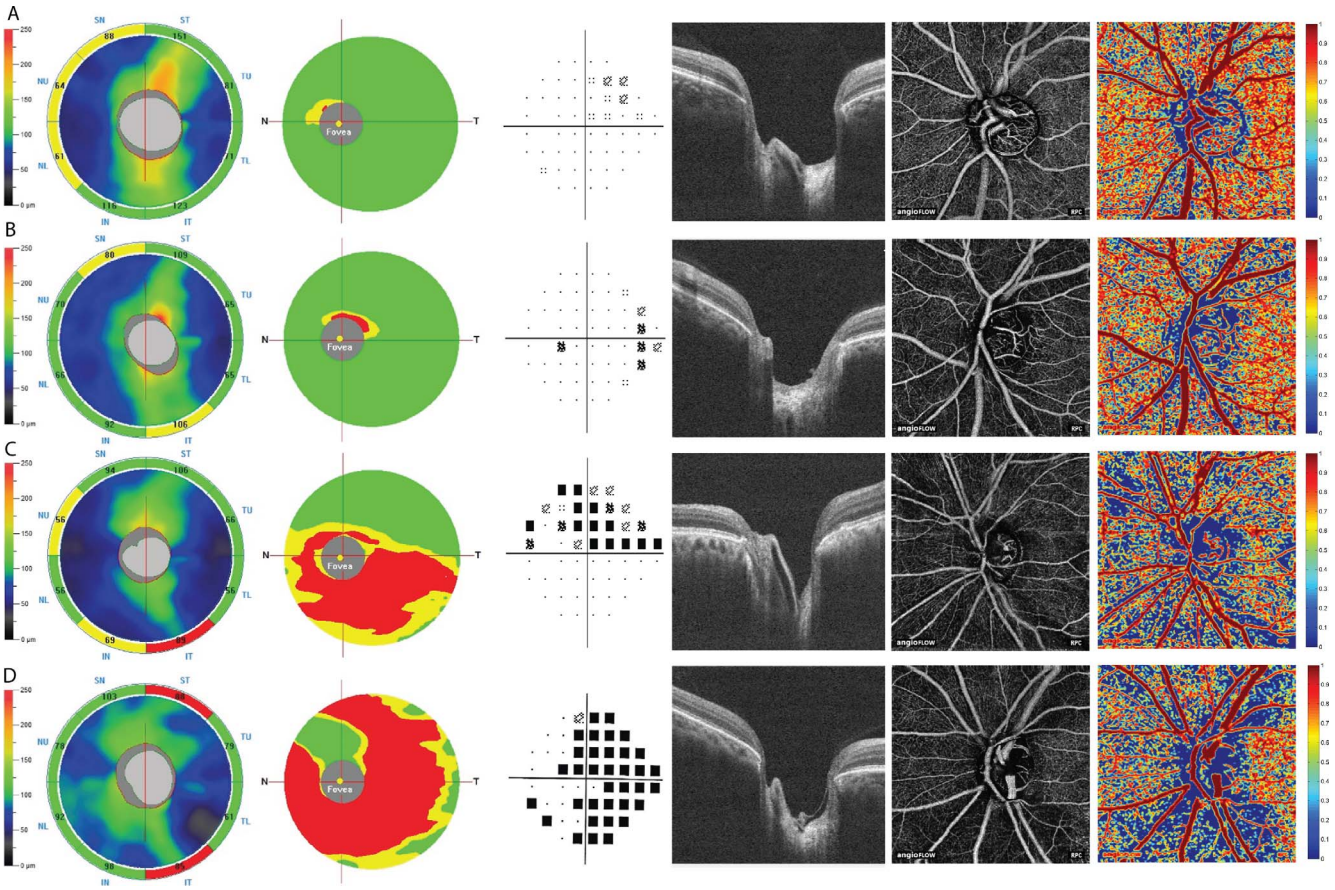

Figure 2. Retinal nerve fiber layer thickness map, GCC map, VF pattern deviation map, structural OCT image, original OCTA of RPC layer, and the corresponding contour map derived from OCTA of (**A**) preperimetric, (**B**) early, (**C**) moderate, and (**D**) severe glaucomatous eye.

Investigative Ophthalmology & Visual Science

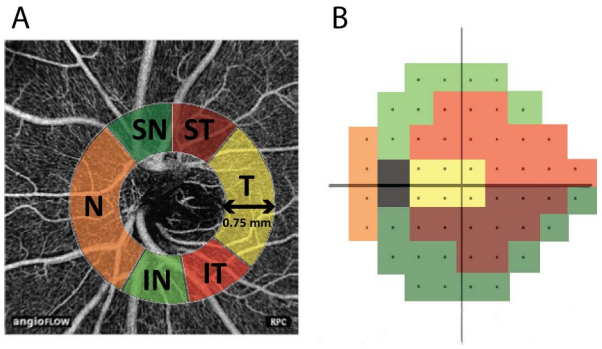

FIGURE 3. (**A**) Optical coherence tomography angiography of RPC layer of glaucomatous eye with the Garway-Heath map sectors (radius = 0.75 mm from the optic disc boundary): T, ST, IT, N, SN, and IN. (**B**) Corresponding Garway-Heath regions on the VF pattern deviation map. The sectors on OCTA image corresponding to the regions in the VF map are depicted in the *same color*.

The image was divided into six sectors (temporal [T], superotemporal [ST], superonasal [SN], nasal [N], inferonasal [IN], and inferotemporal [IT]) around the ONH (radius = 0.75 mm from the ONH boundary) based on Garway-Heath mapping of the VF of an optic disc.[20] Figures 3A and 3B show the OCTA image of the RPC layer with six sectors around the optic disc and the corresponding regions marked with the same color on VF pattern deviation map, using Garway-Heath mapping.[20] Vessel density was expressed in percentage by summing all the pixels with a normalized ratio between 0.7 and 1.0 and then dividing by the total analyzed area of the OCTA image.[16,17] Vessel density was computed for the entire image (vessel density en face), inside the optic disc, and for the six sectors. Similarly, the spacing between large vessels and the spacing between small vessels were expressed as percentage of the total analyzed area of the OCTA image and computed for the entire image and the six sectors. Also, the pattern deviation plot that removed diffuse or generalized field loss and showed only the focal glaucomatous defect was used to compute the regional VF loss. For a given region, the pattern deviation loss was computed by taking an average of the sensitivity loss at each tested point of that region. The pattern deviation loss was computed for all the six VF regions (Fig. 3B).

Statistical Analysis

All analyzed variables were reported as mean along with 95% confidence interval (CI) of the mean. The analyzed variables were vessel density (%), spacing between large vessels (%), spacing between small vessels (%) of the entire image (global vascular parameters) and six sectors (T, ST, SN, N, IN, and IT), and vessel density inside disc (%). One-way analyses of variance were performed between the groups: normal, preperimetric, and glaucomatous eyes for each variable. Linear regressions of global vascular parameters and vessel density inside disc were performed with C/D ratio, RNFL average thickness (μm), GCC average thickness (μm), FLV (%), GLV (%), VF MD (dB), and PSD (dB) for glaucomatous eyes. From a previously established relationship between regional RNFL and GCC loss with VF defects,[21–23] linear regressions of vascular parameters in T, ST, IT, N, SN, and IN sectors were performed with corresponding regional pattern deviation loss in the VF map (Fig. 3). Stepwise logistic regressions were performed by using vascular parameters and VFs. Among the global vascular parameters, vessel density en face and spacing between the large vessels were more susceptible to glaucomatous damage. Regionwise, ST, IT, and SN sectors were more sensitive to vascular changes with the progression of glaucoma than other sectors (T, N, and IN). Similar changes have been observed in a study on pattern of glaucomatous rim loss, which shows loss in IT and ST sectors for early and moderate glaucomatous eyes.[24] There is also pronounced loss in the SN sector in severe glaucomatous eyes.[24] The most affected vascular parameters (global and regional [ST, IT, and SN]) and VFs (MD and PSD) were used to determine the area under the curve (AUC) from logistic regression. Thus, four combinations of variables were used to differentiate between normal, preperimetric, and glaucoma grades: (1) vessel density en face and spacing between large vessels (C1); (2) ST vessel density, IT vessel density, and spacing between large vessels (C2); (3) SN vessel density, IT vessel density, and spacing between large vessels (C3); and (4) VF MD and PSD (C4). The area under the receiver operator characteristic (ROC) curve, sensitivity (%), specificity (%), and likelihood ratios for C1, C2, C3, and C4 were calculated. The Hosmer-Lemeshow statistical test was used to determine the goodness of fit of the logistic regression model.[25] A small χ^2 value (with P value closer to 1) indicated a good logistic regression fit model.[25] Collinearity was examined by variance inflation factor (VIF), and variables with VIF greater than 2 were excluded from the model.[26] A P value < 0.05 was considered statistically significant. All P values were Bonferroni corrected for multiple group comparisons. All statistical analyses were performed in MedCalc v16.2 (MedCalc, Inc., Ostend, Belgium).

Results

Of the 320 eyes (183 patients) that were imaged, 39 eyes had signal strength index less than 40 and were excluded. Of the remaining 281 eyes, eight OCTA images were of poor quality owing to motion artifacts and were excluded. The proportion of subjects with diabetes mellitus was 32%, 35%, 35%, 45%, and 42% in normal, preperimetric, early, moderate, and severe glaucoma grades, respectively (χ^2 test, $P = 0.53$). Also, the proportion of subjects with systemic hypertension was 33%, 21%, 30%, 30%, and 24% in normal, preperimetric, early, moderate, and severe glaucoma grades, respectively (χ^2 test, $P = 0.47$) The proportion of glaucomatous eyes on medications (α-agonist, β-blockers, carbonic anhydrase, and/or prostaglandin analogues) was 25%, 71%, 90%, and 93% in preperimetric, early, moderate, and severe grades, respectively (χ^2 test, $P < 0.0001$).

Ninety-three eyes and 70 eyes had POAG and PACG, respectively. Table 1 shows the demographic and structural characteristics of all the subjects included in the study. All relevant parameters (VF indices [MD and PSD], RNFL [average, superior, and inferior] thickness, GCC [average, superior, and inferior] thickness, GLV [%], and FLV [%]) were significantly altered among the grades of glaucoma ($P < 0.001$; Table 1).

Global Findings

Table 2 shows the vascular parameters: vessel density en face, vessel density inside disc, spacing between large vessels, and spacing between small vessels in the RPC layer of normal and preperimetric, early, moderate, and severe glaucomatous eyes. Normal eyes had a higher vessel density (58.8 [55.8–60.4], $P < 0.001$), higher vessel density inside disc (37.9 [34.5–41.4], $P < 0.001$), lower spacing between large vessels (11.2 [9.9–12.5], $P < 0.001$) and small vessels (30.4 [29.4–31.7], $P < 0.001$) as compared to glaucoma grades (Table 2). Among the glaucoma grades, preperimetric glaucomatous eyes had higher vessel density en face (55.4 [52.3–58.7], $P < 0.001$) and vessel density inside disc (39.8 [37.7–41.8], $P < 0.001$) than early, moderate, and severe glaucomatous eyes (Table 2). Also, the

Table 1. Demographics and Structural Characteristics of Normal, Preperimetric, and Glaucomatous (Early, Moderate, and Severe Glaucoma) Subject Eyes

	Normal (n = 74)	Preperimetric Glaucoma (n = 28)	Early Glaucoma (n = 83)	Moderate Glaucoma (n = 43)	Severe Glaucoma (n = 45)	P Value*	P Value†
Age, y, mean ± SEM	51.2 ± 1.47	57.04 ± 2.78	61.2 ± 1.34	62.6 ± 1.48	61.1 ± 1.19	<0.001‡	0.16
IOP, mm Hg, mean (95% CI)	15.1 (13.7, 16.5)	15.9 (14.7, 17.2)	16.7 (15.6, 17.8)	16.5 (15.0, 18.0)	17.1 (15.9, 18.4)	0.2	0.8
C/D ratio, mean (95% CI)	0.5 (0.47, 0.52)	0.6 (0.53, 0.63)	0.5 (0.52, 0.59)	0.6 (0.56, 0.67)	0.7 (0.61, 0.77)	<0.001‡	0.005‡
MRSE, diopters, mean (95% CI)	0.2 (−0.09, 0.5)	−0.2 (−0.67, 0.16)	0.5 (0.2, 0.7)	−0.08 (−0.6, 0.4)	0.3 (−0.1, 0.7)	0.065	0.035‡
VFI, %, mean (95% CI)	97.2 (96.2, 98.2)	98.2 (97.4, 98.9)	94.0 (93.0, 95.0)	80.3 (76.9, 83.8)	56.2 (48.5, 63.8)	<0.001‡	<0.001‡
VF MD, dB, mean (95% CI)	−2.1 (−2.5, −1.6)	−1.7 (−2.2, −1.1)	−3.2 (−3.6, −2.9)	−8.4 (−9.3, −7.6)	−20.8 (−22.6, −19.1)	<0.001‡	<0.001‡
VF PSD, dB, mean (95% CI)	2.3 (1.9, 2.8)	1.9 (1.5, 2.4)	3.6 (3.2, 4.1)	7.5 (6.4, 8.6)	10.0 (8.9, 11.1)	<0.001‡	<0.001‡
RNFLT average, µm, mean (95% CI)	97.1 (94.8, 99.5)	92.1 (87.6, 96.5)	88.9 (86.1, 91.8)	79.0 (74.9, 83.2)	72.2 (67.3, 77.1)	<0.001‡	<0.001‡
RNFLT superior, µm, mean (95% CI)	118.5 (114.9, 122.1)	113.3 (106.2, 120.3)	107.6 (103.4, 111.8)	97.9 (92.2, 103.6)	87.1 (80.2, 93.9)	<0.001‡	<0.001‡
RNFLT inferior, µm, mean (95% CI)	120.4 (116.9, 123.9)	113.5 (107.1, 119.9)	106.4 (102.1, 110.8)	86.7 (80.5, 92.8)	78.4 (71.6, 85.3)	<0.001‡	<0.001‡
GCCT average, µm, mean (95% CI)	92.9 (90.5, 95.3)	90.9 (87.8, 94.1)	84.9 (81.7, 88.1)	80.2 (76.9, 83.4)	74.6 (70.3, 78.9)	<0.001‡	<0.001‡
GCCT superior, µm, mean (95% CI)	92.1 (89.7, 94.6)	90.4 (87.4, 93.5)	86.4 (83.6, 89.2)	83.5 (80.2, 86.9)	78.7 (73.6, 83.8)	<0.001‡	<0.001‡
GCCT inferior, µm, mean (95% CI)	93.6 (91.2, 96.1)	91.5 (88.2, 94.7)	83.5 (79.1, 87.8)	76.9 (72.9, 80.8)	70.5 (64.6, 76.5)	<0.001‡	<0.001‡
GLV, %, mean (95% CI)	5.4 (3.5, 7.3)	5.9 (3.9, 8.0)	12.9 (10.6, 15.1)	16.1 (13.1, 19.1)	21.7 (17.6, 25.9)	<0.001‡	<0.001‡
FLV, %, mean (95% CI)	1.7 (1.1, 2.3)	2.1 (1.2, 2.9)	4.2 (3.2, 5.3)	5.8 (4.4, 7.2)	8.1 (6.7, 9.5)	<0.001‡	<0.001‡

GCCT, ganglion cell complex thickness; MRSE, manifest refractive spherical equivalent; VFI, visual field index.

* Difference between normal and glaucomatous eyes (overall).

† Difference between preperimetric, early, moderate, and severe glaucomatous eyes.

‡ Indicates significant difference between normal and glaucoma (overall) and between the glaucomatous (preperimetric, early, moderate, and severe) eyes. P value < 0.05 was considered statistically significant.

Table 2. Mean (95% CI) of the RPC Parameters in Normal and Glaucomatous Eyes

	Normal (n = 74)	Preperimetric Glaucoma (n = 28)	Early Glaucoma (n = 83)	Moderate Glaucoma (n = 43)	Severe Glaucoma (n = 45)	P Value*	P Value†
Vessel density en face, %	58.8 (55.8, 60.4)	55.4 (52.3, 58.7)	48.6 (46.8, 50.4)	43.1 (40.2, 45.9)	36.5 (34.1, 39.1)	<0.001‡	<0.001‡
Vessel density inside disc, %	37.9 (34.5, 41.4)	39.8 (37.7, 41.8)	29.8 (27.1, 32.6)	29.8 (25.7, 33.6)	26.7 (23.5, 29.9)	<0.001‡	<0.001‡
Spacing between large vessels, %	11.2 (9.9, 12.5)	11.9 (10.2, 13.8)	16.7 (15.3, 18.1)	22.1 (19.4, 24.6)	29.4 (26.6, 32.1)	<0.001‡	<0.001‡
Spacing between small vessels, %	30.4 (29.4, 31.7)	32.4 (30.9, 33.9)	34.4 (33.7, 35.1)	34.8 (34.1, 35.5)	33.8 (33.1, 34.6)	<0.001‡	0.07

* Difference between normal and glaucomatous eyes (overall).

† Difference between preperimetric, early, moderate, and severe glaucomatous eyes.

‡ Indicates significant difference between normal and glaucoma (overall) and between the glaucomatous (preperimetric, early, moderate, and severe) eyes. P value < 0.05 was considered statistically significant.

Table 3. Pearson's Correlation Coefficient *r* (*P* Value) of Global Vascular Parameters With RNFL, GCC, and VF Parameters in Glaucomatous Eyes

	Vessel Density En Face, %	Vessel Density Inside Disc, %	Spacing Between Large Vessels, %	Spacing Between Small Vessels, %
C/D ratio	−0.37*	−0.32*	0.39*	0.07 (0.39)
RNFLT average, μm	0.61*	−0.01 (0.93)	−0.56*	−0.21 (0.01)
GCCT average, μm	0.44*	0.19 (0.003)	−0.43*	−0.29*
FLV, %	−0.15 (0.08)	−0.002 (0.98)	0.17 (0.04)	0.02 (0.86)
GLV, %	−0.25 (0.003)	0.04 (0.64)	0.25 (0.003)	0.04 (0.64)
VF MD, dB	0.43*	0.04 (0.63)	−0.49*	−0.06 (0.44)
VF PSD, dB	−0.38*	0.07 (0.41)	0.38*	0.10 (0.21)

* Indicates $P < 0.001$. *P* value < 0.05 was considered statistically significant.

spacing between large vessels was significantly higher in moderate (22.1 [19.4–24.6], $P < 0.001$) and severe (29.4 [26.6–32.1], $P < 0.001$) glaucoma grades than in preperimetric (11.9 [10.2–13.8]) and early (16.7 [15.3–18.1]) glaucoma (Table 2). Spacing between small vessels was found to be similar ($P = 0.07$) among the preperimetric and glaucomatous grades (Table 2).

Table 3 gives the Pearson correlation coefficient and significance of the RNFL, GCC, and VF parameters with vascular features. From Table 3, vessel density en face correlated positively with RNFL average thickness ($r = 0.61$, $P < 0.001$), GCC average thickness ($r = 0.44$, $P < 0.001$), and VF MD ($r = 0.43$, $P < 0.001$) and negatively with VF PSD ($r = –0.38$, $P < 0.001$) and C/D ratio ($r = –0.37$, $P < 0.001$). Spacing between large vessels showed a negative correlation with RNFL average thickness ($r = –0.56$, $P < 0.001$), GCC average thickness ($r = –0.43$, $P < 0.001$), and VF MD ($r = –0.49$, $P < 0.001$) and positive correlation with VF PSD ($r = 0.38$, $P < 0.001$) and C/D ratio ($r = 0.39$, $P < 0.001$). Spacing between small vessels showed a negative correlation with RNFL average thickness ($r = –0.21$, $P = 0.01$) and GCC average thickness ($r = –0.29$, $P < 0.001$) (Table 3).Vessel density inside disc showed significant correlation only with C/D ratio ($r = –0.32$, $P < 0.001$) and GCC average thickness ($r = 0.19$, $P = 0.003$) (Table 3).

Regional Findings

Vascular parameters in superior sectors showed a strong correlation with the VF pattern deviation loss in inferior regions and vice versa (Fig. 3). Inferotemporal VF pattern deviation loss correlated with ST vessel density ($r = 0.58$, $P < 0.001$) and spacing between large vessels ($r = –0.57$, $P < 0.001$). Also, ST VF pattern deviation loss showed a good correlation with IT vessel density ($r = 0.64$, $P < 0.001$) and with spacing between large vessels ($r = –0.71$, $P < 0.001$). Superonasal and IN VF loss showed a positive correlation with corresponding IN ($r = 0.31$, $P = 0.001$) and SN ($r = 0.25$, $P = 0.02$) vessel density. Also, SN and IN spacing between large vessels correlated negatively with IN ($r = –0.36$, $P < 0.001$) and SN ($r = –0.41$, $P < 0.001$) VF loss. Spacing between small vessels showed weak correlation with the corresponding regional loss in VF pattern deviation map. Figures 4A and 4B show the en face OCTA image of the optic disc and the structural OCT image of a severe glaucomatous eye. Figures 4C through 4F show the RNFLT, GCC thickness, VF, and OCTA image of RPC layer of a severe glaucomatous eye with the affected or damaged regions marked in red.

Table 4 shows the area under the ROC curve, sensitivity, specificity, and likelihood ratio between normal and preperimetric, early, moderate, and severe glaucomatous eyes, using RNFL average thickness, GCC average thickness, GLV, FLV, and combinations of vascular parameters (C1: vessel density en face and spacing between large vessels; C2: ST and IT vessel density and spacing between large vessels; C3: SN and IT vessel density and spacing between large vessels; C4: VF MD and PSD). The logistic regression model provided a predicted probability of glaucoma when using the combination of variables (C1, C2, C3, and C4).[25] On performing stepwise logistic regression between normal and glaucomatous (overall) eyes, C2 and C4 had a comparable AUC (0.85 and 0.87, respectively, $P = 0.4$). Further, C3 had the best AUC, sensitivity, and specificity (0.70, 69.2%, and 72.9%, respectively) between normal and preperimetric glaucomatous eyes, which was not significantly different ($P = 0.08$) from C4 (0.56, 86.4%, and 40.0%, respectively) (Table 4). C2 had an AUC of 0.82 between normal and early, 0.94 between normal and moderate, and 0.97 between normal and severe glaucomatous eyes (Table 4). These AUC values were comparable ($P > 0.05$) to those of C4 (0.81, 0.97, and 0.99, respectively) (Table 4). Among the combinations of vascular parameters, C2 had the best AUC (0.97) between normal and severe glaucomatous eyes. The logistic regression equation obtained from C2 to differentiate between normal and severe glaucomatous eyes was as follows:

$$\beta = 4.23 + 0.0012\mu_1 + 0.12\mu_2 - 0.11\mu_3 - 0.0033\mu_4. \quad (3)$$

In Equation 3, μ_1 was the IT vessel density, μ_2 was the IT spacing between large vessels, μ_3 was the ST vessel density, and μ_4 was the ST spacing between large vessels. Using Equation 3, a glaucoma severity score (GSS) was computed for normal, preperimetric, and glaucomatous eyes as follows:

$$GSS = \frac{1}{(1 + e^{-\beta})}. \quad (4)$$

Glaucoma severity score provided the probability of the examined eye being a glaucomatous eye, when evaluated with C2. Thus, a score closer to 0 and 1 indicated absence and presence of severe glaucoma, respectively. A GSS between 0 and 1 indicated preperimetric, early, or moderate glaucoma. Glaucoma severity score, using Equations 3 and 4, was applied to normal, preperimetric, and glaucoma grades. Figure 5 shows a bar graph of the mean GSS when using both C2 and C4. Using C2, mean GSS of preperimetric glaucoma (0.19 [0.10–0.28]) was similar ($P > 0.05$) to that of early glaucoma (0.26 [0.22–0.30]). However, preperimetric glaucomatous eyes had significantly different mean GSS from normal (0.01 [0.005–0.02], $P < 0.001$), moderate glaucoma (0.55 [0.47–0.64], $P < 0.001$), and severe glaucoma (0.98 [0.96–1.0], $P < 0.001$). Normal eyes had significantly different ($P < 0.001$) mean GSS, compared to preperimetric and glaucoma grades. Similarly, moderate glaucoma had significantly different ($P < 0.001$) mean GSS from normal, preperimetric, early, and severe glaucoma grades. Also, severe glaucoma had significantly different mean GSS from normal, preperimetric, early, and moderate glaucoma

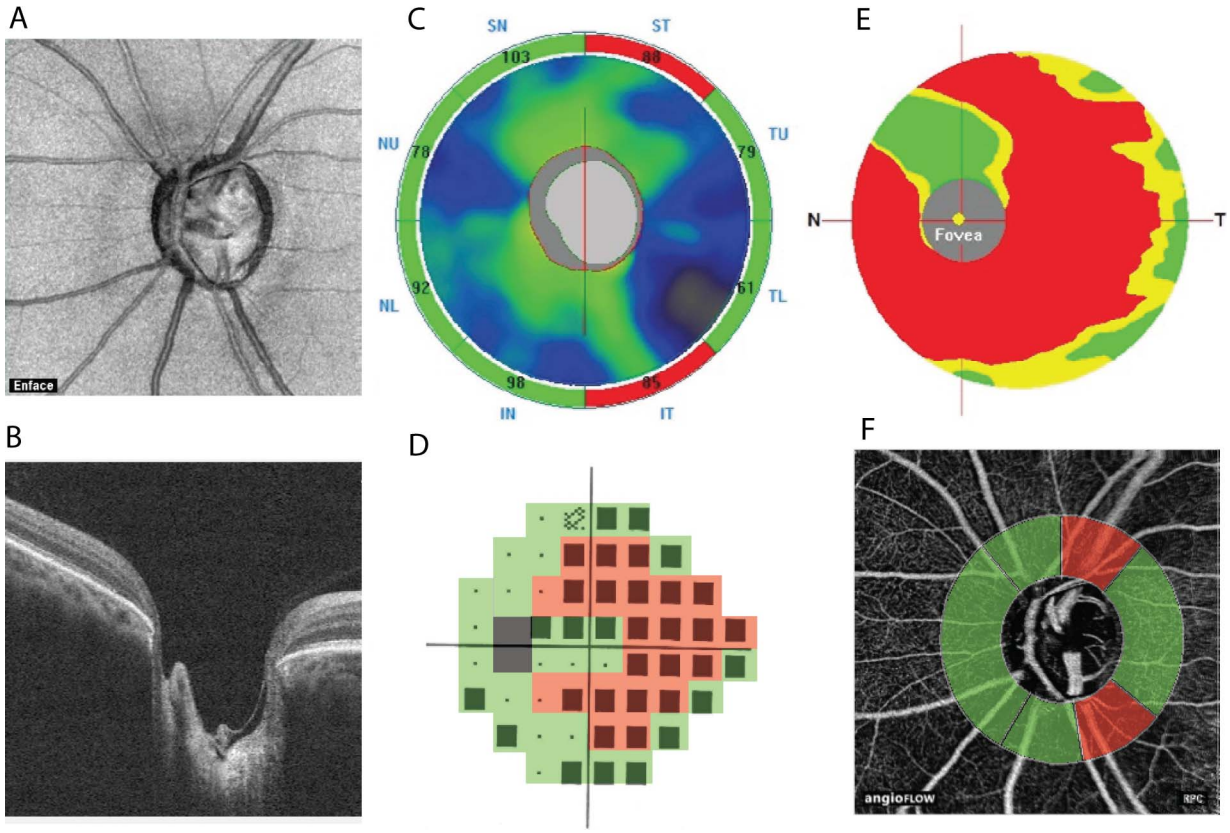

Figure 4. (**A**) En face OCTA image of the optic disc (**B**) structural OCT (image), (**C**) RNFL thickness map, (**D**) VF pattern deviation map, (**E**) GCC map, and (**F**) the corresponding contour map derived from OCTA of RPC layer of a severe glaucomatous eye with the affected/damaged regions shown in *red* (**C**–**F**).

grades. Thus, GSS ranges may be considered as a possible cutoff for grading glaucoma severity.

Discussion

This study confirmed earlier findings on the discriminant capability of the OCTA, based on disease severity using vascular parameters.[7,13–15] Logistic regression was performed by using combinations of global and regional/sectoral vascular parameters to differentiate normal eyes from preperimetric and glaucomatous eyes. These were compared with VFs, RNFL, and GCC parameters. Apart from vessel density en face (global and regional) and vessel density inside disc, the study defined "spaces between large vessels" and "spaces between small vessels." The nomenclature was based on the distribution of vascular network around the ONH. However, further studies and understanding of vascular changes in glaucoma are required to refine these parameters and understand their clinical significance.

Optical coherence tomography angiography is emerging as a useful modality in determining the vascular changes in glaucoma.[7,13,14,27] Recent studies[7,14,15] have shown flow index and vessel density to be significantly lower in eyes with glaucoma than normal eyes, which was also observed in this study (Table 2). Further, this study showed a 22% decrease, 47% increase, and 13% increase in vessel density en face, spacing between large vessels, and spacing between small vessels, respectively, in glaucomatous eyes compared to

Table 4. Logistic Regression of Global and Regional Vascular, RNFL, GCC, FLV, GLV, and Visual Field Parameters With Area Under the ROC Curve (Sensitivity in %, Specificity in %, Likelihood Ratio)

	Normal vs. Preperimetric Glaucoma	Normal vs. Early Glaucoma	Normal vs. Moderate Glaucoma	Normal vs. Severe Glaucoma
RNFLT average, μm	0.66 (77.3, 59.7, 1.91)	0.68 (50, 84.1, 3.14)	0.86 (75, 85.4, 5.13)	0.92 (83.7, 89.7, 7.4)
GCCT average, μm	0.59 (46.2, 76.3, 1.94)	0.74 (78.5, 64.4, 2.21)	0.83 (72.5, 83.1, 4.27)	0.85 (73.3, 94.9, 12.42)
FLV, %	0.57 (31.8, 86.9, 2.42)	0.66 (71.1, 60.5, 1.8)	0.81 (85, 67.9, 2.64)	0.91 (83.3, 91.4, 9.68)
GLV, %	0.55 (36.4, 82.0, 2.02)	0.76 (79.5, 64.2, 2.22)	0.85 (72.5, 84, 4.53)	0.92 (87.5, 90.1, 8.84)
C1	0.62 (68.2, 56.9, 1.58)	0.78 (75.9, 68.2, 2.38)	0.88 (73.2, 88.2, 6.21)	0.92 (76.1, 98.9, 69.2)
C2	0.64 (76.9, 53.3, 1.65)	0.82 (75.9, 81.6, 4.12)	0.94 (80.5, 96.5, 6.57)	0.97 (91.1, 95.3, 19.38)
C3	0.70 (69.2, 72.9, 2.55)	0.81 (62.6, 84.7, 4.09)	0.94 (85.4, 87.1, 6.62)	0.93 (92, 90.6, 9.78)
C4	0.56 (86.4, 40, 1.44)	0.81 (85.2, 69.4, 2.78)	0.97 (92.7, 97.6, 38.62)	0.99 (100, 97.7, 43.47)

C1, combination of vessel density en face and spacing between large vessels; C2, combination of ST and IT vessel density and spacing between large vessels; C3, combination of SN and IT vessel density and spacing between large vessels; C4, combination of visual field MD and PSD.

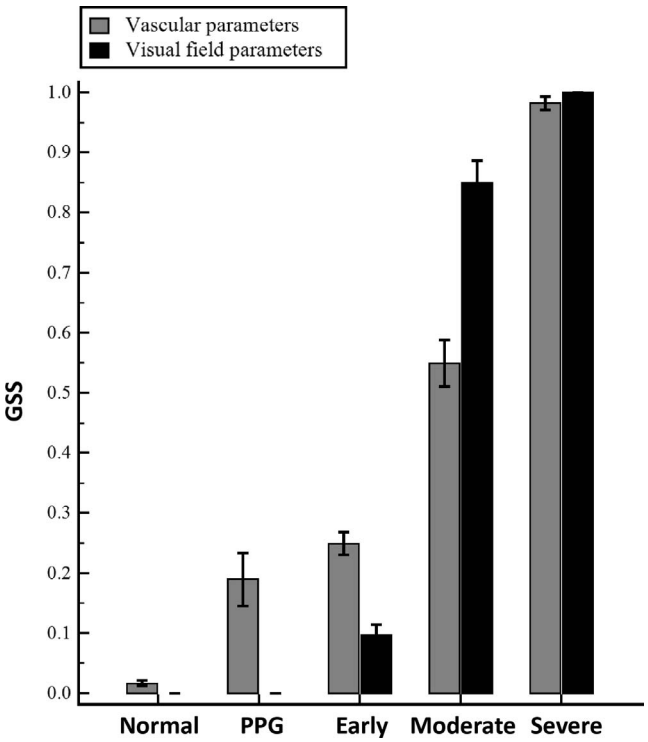

FIGURE 5. Glaucoma severity score derived from stepwise logistic regression using combinations of vascular parameters (C2: ST and IT vessel density and spacing between large vessels) and visual fields (C4: VF mean deviation and pattern standard deviation). Glaucoma severity score provided the probability of the examined eye being a normal, preperimetric glaucoma (PPG), or glaucomatous (early, moderate, or severe) eye. A score closer to 0 indicated a normal eye and closer to 1 indicated severe glaucoma. *Error bars* show the standard error of the mean.

normal eyes. Regionally, ST, IT, and SN sectors showed (1) the maximum decrease in vessel density (24%, 23%, and 29%, respectively); (2) increase in spacing between large vessels (71%, 73%, and 55%, respectively); and (3) increase in spacing between small vessels (31%, 30%, and 14 %, respectively) in glaucomatous eyes compared to normal eyes. Similar results have been reported in a pilot study comparing three normal and three preperimetric glaucoma subjects, where flow index and vessel density were reduced by 35% and by 34%, respectively, in the preperimetric group.[7] A recent study[28] has shown that retinal arterioles are surrounded by a wider capillary-free zone. In this study, the spacing between the large vessels and between small vessels was considered as capillary-free zone in normal eyes. However, the increase in the spacing in the glaucomatous eyes compared to normal eyes is a measure of the increase in the capillary nonperfused area, that is, the spacing between large vessels increased from 11.2% in normal eyes to 16.7% in early glaucoma (Table 2). This 5.5% (16.7–11.2) increase in spacing could indicate an increase in capillary nonperfusion in early glaucomatous eyes. A corresponding decrease was observed in capillary perfusion (vessel density en face decreased from 58.8% in normal eyes to 48.6% in early glaucomatous eyes). A similar trend has also been observed in spacing between the large vessels in a recently published study on diabetic retinopathy using OCTA.[16]

Visual field (MD and PSD) and OCT parameters (RNFL and GCC) are widely used to differentiate glaucomatous eyes from normal eyes.[21,22] In this study, the ROC curve results (AUC, sensitivity, and specificity) of these parameters were comparable to those of previous studies (Table 4).[21,29] To compare the diagnostic ability of OCTA with the current clinical standards, previous studies[14,15] have correlated vessel density with structural (RNFL and GCC) and functional (VF MD and PSD) parameters. A study on peripapillary retina in glaucoma has shown a strong correlation of vessel density ($r = –0.86$, $P < 0.001$) with the stage of glaucoma (based on the Enhanced Glaucoma Staging System).[15] This is comparable to the correlation with VFMD ($r = 0.68$, $P = 0.02$) and VF PSD ($r = –0.84$, $P = 0.001$).[15] Another study on correlation of optic disc perfusion with severity of glaucoma has shown a significant correlation of vessel density with VF MD ($r = 0.41$, $P = 0.001$), VF PSD ($r = –0.25$, $P = 0.049$), RNFLT ($r = 0.465$, $P < 0.001$), and GCC thickness ($r = 0.45$, $P < 0.001$).[14] These findings match up with the results of the current study, which showed significant correlation of vessel density en face with VF MD ($r = 0.43$, $P < 0.001$), VF PSD ($r = –0.38$, $P < 0.001$), RNFLT ($r = 0.61$, $P < 0.001$), and GCC thickness ($r = 0.44$, $P < 0.001$). As expected, spacing between large vessels also showed significant correlation with VF MD ($r = –0.49$, $P < 0.001$), VF PSD ($r = 0.38$, $P < 0.001$), RNFLT ($r = –0.56$, $P < 0.001$), and GCC thickness ($r = –0.43$, $P < 0.001$). However, all these were global correlations. Previous studies[22,23,30] have already established regional correlations between RNFL loss, GCC loss, and VF deficits. This study looked at sectoral vascular changes with corresponding regional VF defects. A study on vascular changes in glaucoma has shown superior VF loss matching with inferior vessel density and vice versa,[15] demonstrating the relationship between regional vascular changes and VF defects. Similar results were also observed in this study, which showed a strong correlation between (1) ST and IT vessel density ($P < 0.001$ each) and (2) spacing between large vessels ($P < 0.001$ each) and the corresponding IT and ST VF loss. Superonasal and IN vascular parameters also showed a good correlation ($P < 0.05$) with IN and SN VF loss. These observations demonstrate the capability of OCTA in detecting global and regional glaucomatous vascular damage with the corresponding regional VF damage.

In a recent study,[14] AUC of the flow index and vessel density was reported to be 0.80 and 0.82, respectively. The AUC was 0.9 for both parameters, when normal eyes are compared with severe glaucoma.[14] Another study[15] reported an AUC of 0.89 and 0.94 for flow index and vessel density between normal and glaucomatous eyes, respectively. To improve the discriminant ability of OCTA, different combinations of vascular parameters were used in this study. The combinations were selected on the basis of the most susceptible vascular parameters to glaucomatous damage. Globally, vessel density en face and spacing between large vessels showed significant change with disease severity compared to normal eyes (Table 2). The ONH vascular network was similar ($P > 0.05$) among the glaucoma grades (early, moderate, and severe). Also, the spacing between small vessels was similar ($P > 0.05$) among the preperimetric and glaucoma grades. Regionally, ST, SN, and IT sectors showed maximum loss in vessel density with the progression of glaucoma. Similar pattern of regional loss of the neuroretinal rim with glaucoma progression has been reported in a previous study.[24] Using stepwise logistic regression, C1 (combination of global vessel density and spacing between large vessels), C2 and C3 (sectorwise density and spacing) offered the best AUC fits (Table 4). All three combinations (C1, C2, and C3) resulted in comparable AUCs ($P > 0.05$) to both functional (C4) and structural parameters (RNFL and GCC) for preperimetric and glaucoma grades (Table 4). By using the logistic regression equation derived with C2, a GSS was proposed to help determine if a subject's eye was normal, preperimetric, or glaucomatous (Fig. 5). Vascular parameters (C2) appeared to show a GSS very close to 0 for normal eye and close to 1 for

severe glaucomatous eyes. Preperimetric, early, and moderate glaucomatous eyes have a clear incremental GSS value between 0 and 1 (Fig. 5). However, the VF parameters (C4) showed a GSS of 0 for both normal and preperimetric glaucoma. This was expected, as functional damage (in the form of VF loss) was absent in the preperimetric stage. Also, the GSS for early glaucoma with regard to VF criteria was lower than vascular parameters, as fields are minimally damaged in early glaucoma. This indicated that the structural/vascular damage happens before functional damage, which has been demonstrated in previous studies using RNFL and GCC measurements.[21] However, GSS was higher (or comparable) owing to severe functional damage in moderate and severe glaucoma. Thus, GSS may have the potential of increasing the detection of true preperimetric and early glaucoma as compared to VF criteria.

This study had a few limitations. A previous study on OCTA images of 55 normal eyes of Indian patients between 20 to 67 years of age, using the fractal-based method described in this study, has demonstrated that vessel density did not significantly decrease with increase in age.[16] In this study, age did not have a significant effect on vessel density en face ($r = -0.09$, $P = 0.44$), spacing between large vessels ($r = 0.1$, $P = 0.41$), and spacing between small vessels ($r = 0.08$, $P = 0.52$) in normal eyes. This is contrary to recent studies that have shown a significant decrease in vessel density with age.[31,32] Also, vascular parameters were found to be similar ($P > 0.05$) with increase in age in preperimetric glaucomatous eyes. From these observations, age difference between normal and glaucomatous eyes was not considered in the analysis. However, further understanding of the effect of age on vascular parameters in a large cohort of Indian eyes is needed and will be evaluated in future studies. The smaller sample size in the preperimetric group may have precluded finding larger differences from normal eyes. This study also did not include glaucoma suspects, which could have altered the diagnostic strength of the device and analyses technique. Further, all glaucoma subjects included in this study were on topical ocular medications for IOP control. While some topical medications may increase blood flow, there are no appropriate tools or end points to quantify the effect of medications on blood flow or vascular parameters.[33] Further, most IOP medications have been shown to increase perfusion in the ONH.[33,34] Also, details about systemic medications were not captured. Lack of data on systemic parameters such as blood pressure and mean ocular perfusion pressure can be possible confounders. However, no correlation between systemic parameters and vessel density in normal or glaucomatous eyes has been established yet.[15] Inter- and intravisit repeatability was not checked; however, previous studies[12,13] have already demonstrated good repeatability for both criteria.

The spacing between small vessels did not show any significant differences between normal and glaucomatous eyes, nor did it show any specific correlations with clinical parameters. Studying the spacing between small vessels could be challenging and confounding. As the OCTA images used in this study had a resolution of 304×304 pixels over a 4.5×4.5-mm scan area, it is possible that a spacing smaller than the resolution of the pixel may not be seen on the OCTA images. Further, this is also dependent on image acquisition speeds, and faster imaging may show fewer small vessels.[35] It is possible that this technology limitation precludes the detection of a significant difference for spacing between small vessels among the glaucoma grades. Further, it is also possible that with progression of glaucoma and increase in capillary dropout, a few but an insignificant number of the smaller spacings may gradually transition into larger spacings. Longitudinal assessment of the same eye prospectively can possibly help in understanding this trend better. The OCTA software can introduce artifacts such as loss of detail, doubling of vessels, stretching defects, and false-flow artifact.[36] Despite techniques used to compensate for axial eye motions, transverse motions from fixation changes remain a major cause of artifacts in OCTA.[36] However, with increased OCT scanning speeds and subsequent decreased imaging time, the problem of motion artifacts can be reduced to a certain extent. In this study, OCTA images with significant motion artifacts or stretching defects or doubling of vessels were excluded. However, other artifacts that were not apparent could have some confounding effect on the results of this study. Studies[28,37] have also reported autosegmentation errors and projection artifacts in the deep macular plexus with OCTA software. However, projection artifacts are only seen in the structures present below the vasculature. Thus, the OCTA images of the RPC layer had no such errors. Another limitation was the lack of awareness of the dynamic range of the technology; the highest/lowest value beyond which the device cannot accurately measure flow or vessel density was not known.[35]

Vascular parameters appear to be a useful new noninvasive adjunct tool to evaluate/diagnose glaucoma. They appear to correlate well with functional and structural clinical parameters. It is not clear at this time if vascular changes are a cause or effect of glaucoma. Longitudinal studies are needed to determine the usefulness of this tool in early detection of disease and prognostication.

Acknowledgments

Disclosure: **R.S. Kumar**, None; **N. Anegondi**, None; **R.S. Chandapura**, None; **S. Sudhakaran**, None; **S.V. Kadambi**, None; **H.L. Rao**, None; **T. Aung**, None; **A. Sinha Roy**, None

References

1. Hyman L, Wu SY, Connell AM, et al. Prevalence and causes of visual impairment in The Barbados Eye Study. *Ophthalmology*. 2001;108:1751–1756.
2. Quigley HA, Broman AT. The number of people with glaucoma worldwide in 2010 and 2020. *Br J Ophthalmol*. 2006;90:262–267.
3. Flammer J. The vascular concept of glaucoma. *Surv Ophthalmol*. 1994;38(suppl):S3–S6.
4. Flammer J, Orgul S, Costa VP, et al. The impact of ocular blood flow in glaucoma. *Prog Retin Eye Res*. 2002;21:359–393.
5. Harris A, Rechtman E, Siesky B, et al. The role of optic nerve blood flow in the pathogenesis of glaucoma. *Ophthalmol Clin North Am*. 2005;18:345–353.
6. Francois J, de Laey JJ. Fluorescein angiography of the glaucomatous disc. *Ophthalmologica*. 1974;168:288–298.
7. Jia Y, Morrison JC, Tokayer J, et al. Quantitative OCT angiography of optic nerve head blood flow. *Biomed Opt Express*. 2012;3:3127–3137.
8. Petrig BL, Riva CE, Hayreh SS. Laser Doppler flowmetry and optic nerve head blood flow. *Am J Ophthalmol*. 1999;127:413–425.
9. Riva CE. Basic principles of laser Doppler flowmetry and application to the ocular circulation. *Int Ophthalmol*. 2001;23:183–189.
10. Sugiyama T, Araie M, Riva CE, et al. Use of laser speckle flowgraphy in ocular blood flow research. *Acta Ophthalmol*. 2010;88:723–729.
11. Tan O, Wang Y, Konduru RK, et al. Doppler optical coherence tomography of retinal circulation. *J Vis Exp*. 2012;e3524.

12. Jia Y, Tan O, Tokayer J, et al. Split-spectrum amplitude-decorrelation angiography with optical coherence tomography. *Opt Express*. 2012;20:4710–4725.
13. Jia Y, Wei E, Wang X, et al. Optical coherence tomography angiography of optic disc perfusion in glaucoma. *Ophthalmology*. 2014;121:1322–1332.
14. Wang X, Jiang C, Ko T, et al. Correlation between optic disc perfusion and glaucomatous severity in patients with open-angle glaucoma: an optical coherence tomography angiography study. *Graefes Arch Clin Exp Ophthalmol*. 2015;253:1557–1564.
15. Liu L, Jia Y, Takusagawa HL, et al. Optical coherence tomography angiography of the peripapillary retina in glaucoma. *JAMA Ophthalmol*. 2015;133:1045–1052.
16. Bhanushali D, Anegondi N, Gadde SG, et al. Linking retinal microvasculature features with severity of diabetic retinopathy using optical coherence tomography angiography. *Invest Ophthalmol Vis Sci*. 2016;57:OCT519–OCT525.
17. Gadde SG, Anegondi N, Bhanushali D, et al. Quantification of vessel density in retinal optical coherence tomography angiography images using local fractal dimension. *Invest Ophthalmol Vis Sci*. 2016;57:246–252.
18. Susanna R Jr, Vessani RM. Staging glaucoma patient: why and how? *Open Ophthalmol J*. 2009;3:59–64.
19. Taud H, Parrot J-F. Measurement of DEM roughness using the local fractal dimension. *Géomorphologie*. 2005;10:11.
20. Garway-Heath DF, Poinoosawmy D, Fitzke FW, Hitchings RA. Mapping the visual field to the optic disc in normal tension glaucoma eyes. *Ophthalmology*. 2000;107:1809–1815.
21. Kim NR, Lee ES, Seong GJ, et al. Structure-function relationship and diagnostic value of macular ganglion cell complex measurement using Fourier-domain OCT in glaucoma. *Invest Ophthalmol Vis Sci*. 2010;51:4646–4651.
22. Le PV, Tan O, Chopra V, et al. Regional correlation among ganglion cell complex, nerve fiber layer, and visual field loss in glaucoma. *Invest Ophthalmol Vis Sci*. 2013;54:4287–4895.
23. Wu H, de Boer JF, Chen L, Chen TC. Correlation of localized glaucomatous visual field defects and spectral domain optical coherence tomography retinal nerve fiber layer thinning using a modified structure-function map for OCT. *Eye (Lond)*. 2015;29:525–533.
24. Jonas JB, Fernandez MC, Sturmer J. Pattern of glaucomatous neuroretinal rim loss. *Ophthalmology*. 1993;100:63–68.
25. Bewick V, Cheek L, Ball J. Statistics review 14: logistic regression. *Crit Care*. 2005;9:112–118.
26. O'Brien RM. A caution regarding rules of thumb for variance inflation factors. *Quality Quantity*. 2007;41:673–690.
27. Hollo G. Vessel density calculated from OCT angiography in 3 peripapillary sectors in normal, ocular hypertensive, and glaucoma eyes. *Eur J Ophthalmol*. In press.
28. Bonnin S, Mane V, Couturier A, et al. New insight into the macular deep vascular plexus imaged by optical coherence tomography angiography. *Retina*. 2015;35:2347–2352.
29. Huang JY, Pekmezci M, Mesiwala N, et al. Diagnostic power of optic disc morphology, peripapillary retinal nerve fiber layer thickness, and macular inner retinal layer thickness in glaucoma diagnosis with fourier-domain optical coherence tomography. *J Glaucoma*. 2011;20:87–94.
30. Danthurebandara VM, Sharpe GP, Hutchison DM, et al. Enhanced structure-function relationship in glaucoma with an anatomically and geometrically accurate neuroretinal rim measurement. *Invest Ophthalmol Vis Sci*. 2015;56:98–105.
31. Shahlaee A, Samara WA, Hsu J, et al. In vivo assessment of macular vascular density in healthy human eyes using optical coherence tomography angiography. *Am J Ophthalmol*. 2016;165:39–46.
32. Yu J, Jiang C, Wang X, et al. Macular perfusion in healthy Chinese: an optical coherence tomography angiogram study. *Invest Ophthalmol Vis Sci*. 2015;56:3212–3217.
33. Seong GJ, Lee HK, Hong YJ. Effects of 0.005% latanoprost on optic nerve head and peripapillary retinal blood flow. *Ophthalmologica*. 1999;213:355–359.
34. Arend O, Harris A, Arend S, et al. The acute effect of topical beta-adrenoreceptor blocking agents on retinal and optic nerve head circulation. *Acta Ophthalmol Scand*. 1998;76:43–49.
35. Schuman JS. Measuring blood flow: so what? *JAMA Ophthalmol*. 2015;133:1052–1053.
36. Spaide RF, Fujimoto JG, Waheed NK. Image artifacts in optical coherence tomography angiography. *Retina*. 2015;35:2163–2180.
37. Zhang M, Hwang TH, Campbell JP, et al. Projection-resolved optical coherence tomographic angiography. *Biomed Opt Express*. 2016;7:816–828.

Investigative Ophthalmology & Visual Science